Jurnal Inovasi Pendidikan dan Sains
Vol.5 No.3, Desember 2024: 148-154 ISSN 2721-9119 (Online)

PHOTOCATALYTIC DEGRADATION OF METHYLENE BLUE (MB) BY CERIUM DOPED TITANIUM DIOXIDE (Ce/TiO_2) UNDER UV-VISIBLE LIGHT IRRADIATION

Adi Gunawan[1]

[1] Program Study Agricultural engineering, Faculty of Agriculture, Muhammadiyah University of Mataram, Indonesia

*Email: adigunbio@gmail.com

Accepted: October 23th 2024 Approved: 20th December 2024. Published: 27th December 2024

Abstract: Photocatalytic degradation of MB was applied using Ce-doped TiO_2 under UV-visible light irradiation. The aim of this investigation is to improve the light absorption ability of Ce-doped TiO_2 under UV-visible light irradiation to degradation of MB. The TiO_2 catalyst was provided by the sol-gel method and addition doping of Ce with 1wt%, 2wt%, 3wt%, 4wt%, and 5wt% concentration. The characterization of photocatalyst has been observed through XRD, UV-vis spectroscopy, PL, and nitrogen absorption. Measurement of UV-Visible absorption showed that increased in dopant concentration in the range 1wt%–5wt% decreased the optical band gap of Ce-doped TiO_2. Photocatalyst with doping 3wt% concentration of Ce showed the best photocatalytic activity. The effect of addition Ce successfully to prevent the growth of anatase phase TiO_2, enhanced of surface area and enhanced the optical properties of TiO_2. The result was effective to prevent the electron-hole recombination and increase the ability of photocatalytic activity in degrade of MB.

Keywords: diversity, orthoptera, purposive sampling

INTRODUCTION

Textile dye is one of the biggest organic compounds that cause environmental hazards. Estimated that over 10,000 different dyes and pigments are used industrial and 50% consist of textile dye [1][2]. The direct discharge of dyes leads to hazardous effects on the environment, public health and ecosystems [3][4]. Textile effluents contain a large variety of dyes such as Rhodamine B, methyl red, methyl orange and MB. These types of dye can cause irritations to the skin and eyes, growth reduction, neurosensory damage and death. Hence, effective processing of textile effluent before discharge into the environment is most important.

Photocatalytic process is an effective way to degrade dyes in the environment. Photocatalytic technique can be used to degrade the concentration of dyes such as MB in wastewater before discharge into the environment[5]. Titanium dioxide (TiO_2) is one of the semiconductor for the degradation of organic contaminants in water. In addition, TiO_2 is generally used as a catalyst because are abundant in nature, inexpensive, non-toxic, has strong reduction properties, and high photostability[6][7][8].

However, non-modified TiO_2 has the weakness of large bandgaps, fast recombination of electrons and holes, and only responsive in UV light. To resolves this weakness, TiO_2 semiconductor are doped with metal ion or oxides. Doping of TiO_2 could increase the photocatalytic efficiency and the absorbance for visible light irradiation [9][10][7][11][12][13][14]. Cerium in metals in the lanthanide series has been used because of the catalytic and optical properties associated with the redox pair Ce^{3+}/Ce^{4+}.

The reports of TiO_2 doped with Cerium to degrade MB are still limited. In recent years, the photocatalytic activity of TiO_2 has been increased with the incorporation of cerium [15] and tested in photodegradation of various pollutant models, such as Phenols, chlorophenol to probe the light absorption ability and the effects of doping on the photocatalytic activity[16]. The aim of this investigation is to improve the light absorption ability of Ce-doped TiO_2 under UV-visible light irradiation to degradation of MB.

RESEARCH METHODS

1. Material

Glacial acetic acid and absolute ethanol were purchased from Merck and Fisher, respectively. Cerium (III) nitrate hexahydrate ($Ce(NO_3)_3.6H_2O$) and Titanium (IV) n-butoxide were purchased from Fluka and Acros, respectively. Methylene Blue (MB) were purchase from Ricca. All the chemicals were used without further purifying and Distilled water was used for whole test.

2. Preparation of TiO_2 and cerium/ TiO_2

The synthesis methods of Ce/TiO_2 are using a modified sol-gel method with the following steps. Preparation of solution A, 5 ml of glacial acetic acid and 10 ml of absolute ethanol are added to 10 ml of Titanium (IV) n-butoxide with continuous stirring. Preparation of solution B, 4 ml deionized water with an appropriate amount of Cerium (III) hexahydrate nitrate, 6 ml of acetic acid and 30 ml of ethanol. Then Solution A is dripped into solution B with constant stirring for 30 minutes. The solution is closed then heated at the temperature 60°C for 2 hours under continuous stirring (stirring speed = 500 rpm). The gel result then dried in the oven at 80°C for 12 hours. The dry sample then washed with distilled water to remove the non-reactant chemicals after which it is dried again at 80°C for 12 hours. Dry samples were mashed using agate mortar and calcined in a muffle furnace at the temperature 450°C with a heating rate of 1°C / min for 4 hours. The samples are labelled as x Ce/TiO_2, where x is the amount of Ce concentration for doping TiO_2 (x = 1wt%, 2wt%, 3wt%, 4wt%, 5wt%).

3. Characterization of photocatalyst

The photocatalyst crystal structure produced by Ce/TiO_2 synthesis was identified using X-ray diffractometer (XRD) Siemens 2000x series that recorded in the range $2\theta = 20\text{-}90$ with Cu-kα radiation (λ = 1.5406 Å), counted by using the Scherrer equation, $D = K\lambda / \beta \cos\theta$. where D is the average

crystallite size (nm), K is the Scherrer constant (0.89), λ is the wavelength of the X-ray source, β is the full width at half maximum and θ is the angle Bragg. The Vis Diffuse Reflectance Spectra (Vis DRS) that used to analyze the band gap energy of the TiO_2 were recorded by using the Perkin Elmer Lambda 35 UV-vis spectrophotometer in the range of 300-800 nm with the Kubelka-Munk function.

Photoluminescence (PL) spectroscopy was operated by the Perkin Elmer Lambda S55 spectrofluorometer using Xe lamps with excitation wavelengths of 290 nm. Nitrogen (N2) adsorption-desorption isotherm were recorded by using a Micromeritics ASAP 2020 surface analyzer to obtain the characteristics and BET surface area, pore diameter, pore volume and band gap energy.

4. Photocatalytic activity experiment

Experiments of photocatalytic activity were carried out in a UV-Vis irradiation of light 120 W. The photodegraded solution was MB solution prepared with distilled water. Photocatalytic reaction using a slurry suspension made by adding 1 g/L of TiO_2 nano powder doped with TiO_2 into the MB solution. Process parameters will be evaluated using different amount of catalyst (1wt%, 2wt%, 3wt% and 5wt%). To assure an adsorption / desorption balance between the catalyst and solution, the MB solution catalysts are stirred for 1 hour in the dark. During the photocatalytic reaction the MB solutions are blown using air and irradiated using a 120 W lamp positioned above the reactor. the MB solution catalyst will be withdrawn periodically (~ 2mL) based on predetermined irradiation time intervals. The MB solutions were pulled out and analyzed to determine it is concentrations. The concentration of MB the solution was analyzed by a UV-VIS spectrophotometer with maximum absorbance at 600 nm.

RESULTS AND DISCUSSION

1. XRD analysis for Ce/TiO_2 photocatalysts

The XRD pattern for Ce/TiO_2 with different Cerium content is shown in Figure 1**.** Based on the XRD analysis that, the diffraction spectra for all the photocatalysts only to the anatase phase composition. The diffraction peaks around 2θ = 25.3, 37.7, 48.2 53.9, 55.1 and 62.7 are identified and can be attributed to the diffraction faces of (101), 166 (004), (200), (105), (211) and (204) anatase TiO_2. For the modified photocatalysts such as Ce-doped TiO_2, it was observed there is no metal oxide were found or no diffraction peaks of the phases accommodate Ce were found, which showed that Ce^{3+} ions substituted the interstitial sites in TiO_2 lattice or a good dispersion of the metal species [17].

Based on the research conducted at the Institut Teknologi Sumatera (ITERA), 12 genera were found at four observation station points. At Station I, 161 individuals were found; at Station II, 204 individuals were found; at Station III, 136 individuals were found; and at Station IV, 145 individuals were found (Table 1)

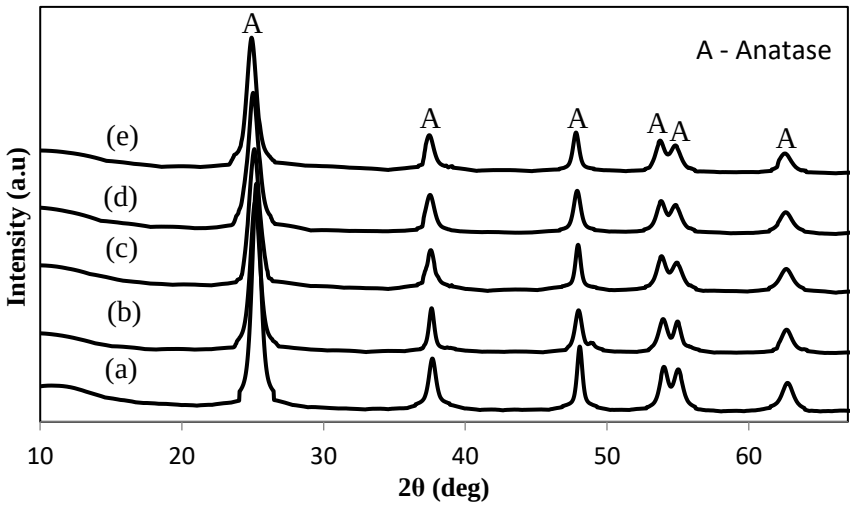

Figure 1. XRD patterns of Ce doped TiO_2 photocatalysts (a) TiO_2, (b) 1wt% Ce/TiO_2, (c) 2wt% Ce/TiO_2, (d) 3wt% Ce/TiO_2 and (e) 5wt% Ce/TiO_2

Table 1. Crystallite size for Ce doped TiO_2 photocatalysts

Photocatalyst	Crystallite size, $<D>_v$ (nm)
Pure TiO_2	17.40
1wt% Ce/TiO_2	13.64
2wt% Ce/TiO_2	12.63
3wt% Ce/TiO_2	12.23
5wt% Ce/TiO_2	12.57

It can be seen that size of TiO_2 crystals decreases with increasing doping content. The most significant reduction in crystallite size was concentration 3wt% of Ce/TiO_2 with the smallest

crystallite size being 12.23 nm. It is indicated that crystallite growth is inhibited by the presence doping of Ce [18]. These catalysts indicate the anatase phase with a small particle size. It was indicated that the addition of Ce could prevent the growth of TiO_2 crystalline and phase transformation.

The reduction in crystal size is due to the Ce-O-Ti linkages formed on the surface and the interstitial site of the catalyst sample, thereby inhibit the growth of crystal granules (Stengl et al., 2009).

2. UV-vis DRS analysis for Ce/TiO_2 photocatalysts

The absorption wavelength for Ce/TiO_2 photocatalysts and pure TiO_2 determined using the UV–Vis analysis in **Figure 2.**

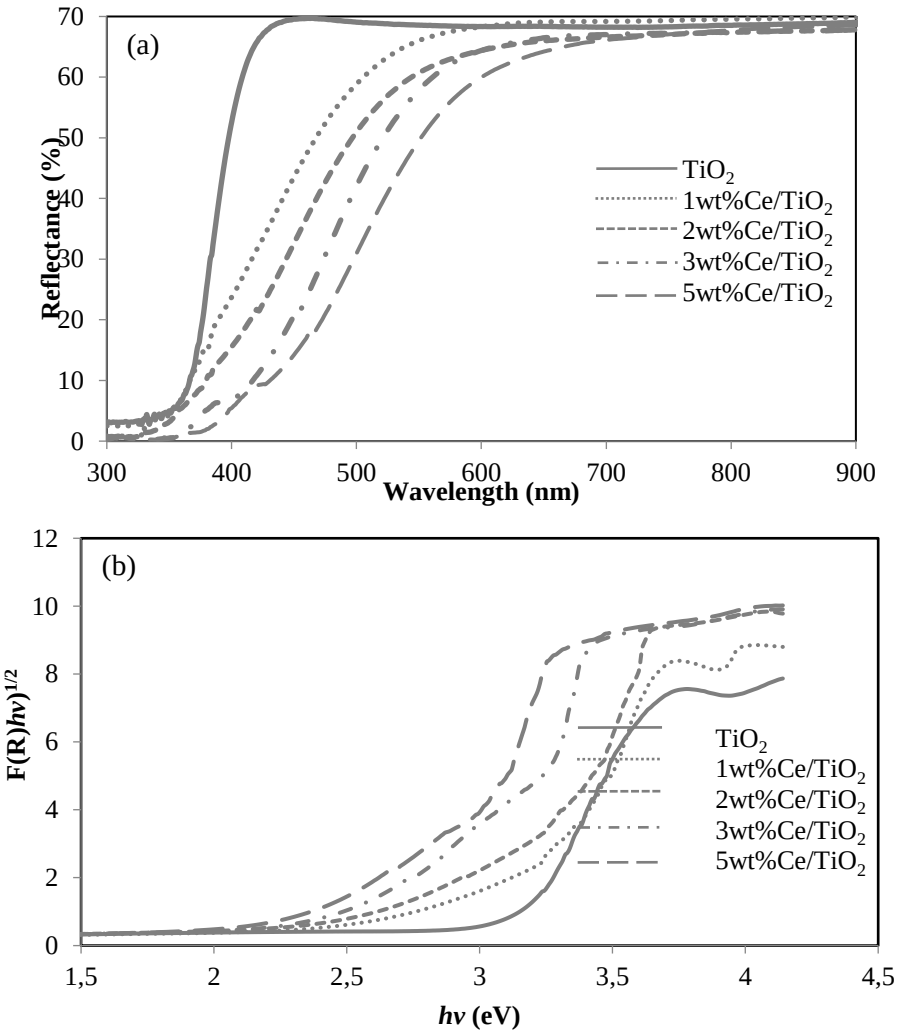

Figure 2. Diffuse reflectance spectra and (b) Kubelka-Munk function for TiO_2 and Ce doped TiO_2 photocatalysts

Additional of Ce doping content increases the absorption capability of Ce/TiO_2 light and results in a redshift from the absorption edge towards the visible light area. The redshift explains the presence of Ti-O-Ce bonds and produce new energy levels in the band gap and thus, decrease the band gap energy of Ce/TiO_2 [19]. **Figure 2** (b) shows the Kubelka-Munk plot for Ce/TiO_2 photocatalysts. On the other hand, concentrate cerium contributes for resulted of electron holes pairs under UV visible light irradiation.

3. Photoluminescence (PL) analysis for Ce/TiO_2 photocatalysts

The PL spectra for Ce/TiO_2 photocatalysts and pure TiO_2 are showed in **Figure 3.** The PL analysis has been widely used to explain energy transfer rate, doping concentration and the efficiency of the segregate of electron hole pairs [20][21][22]. Based on observations, the two photoelectron peaks on all catalysts has similarity shape and position of energy. This indicates that added Ce ions did not lead to new light emitting phenomenon.

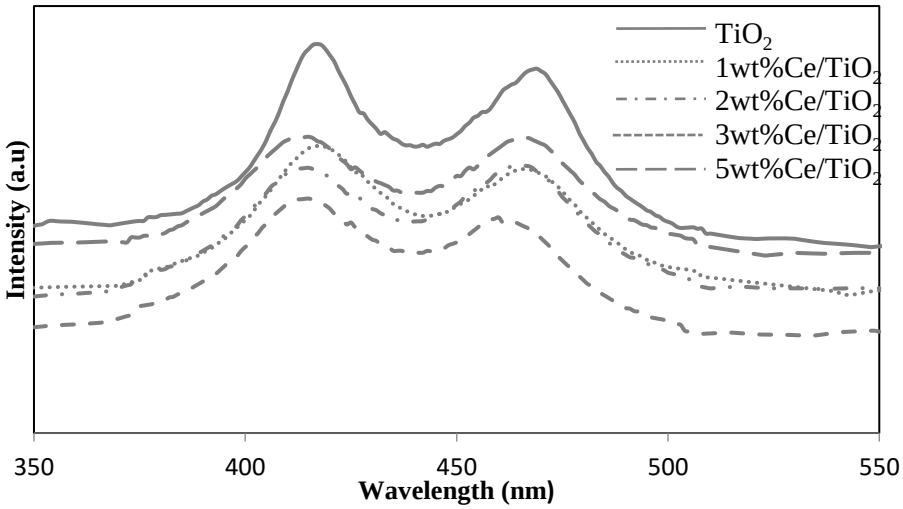

Figure 3. PL spectra for pure and Ce doped TiO_2 photocatalysts

Increased Cerium concentration (i.e. 1wt%, 2wt% and 3wt%) causes a decrease the PL spectrum intensity and with doping 3wt% of Ce showed the weakest PL spectrum. Decrease of the PL spectrum intensity probably caused due to the merger of Cerium ions into the catalyst lattice [23]. Increased semiconductor photocatalytic activity caused electrons and holes take part in oxidation reduction reactions [24][23]. This shows that Ce/TiO_2 has reduced recombination rate, enhanced charge separation in the photocatalyst properties and leads to better photocatalyst response [25][26]. In conclusion, the low intensity of the PL spectrum shows the higher the photocatalytic activity and indicated the best photocatalytic activity.

4. N_2 adsorption-desorption isotherm for Ce/TiO_2 photocatalysts

Figure 4. showed N_2 adsorption–desorption isotherms of the pure TiO_2 and Ce/TiO_2. nitrogen sorption measurement to decide the surface characteristic of Ce/TiO_2 photocatalyst.

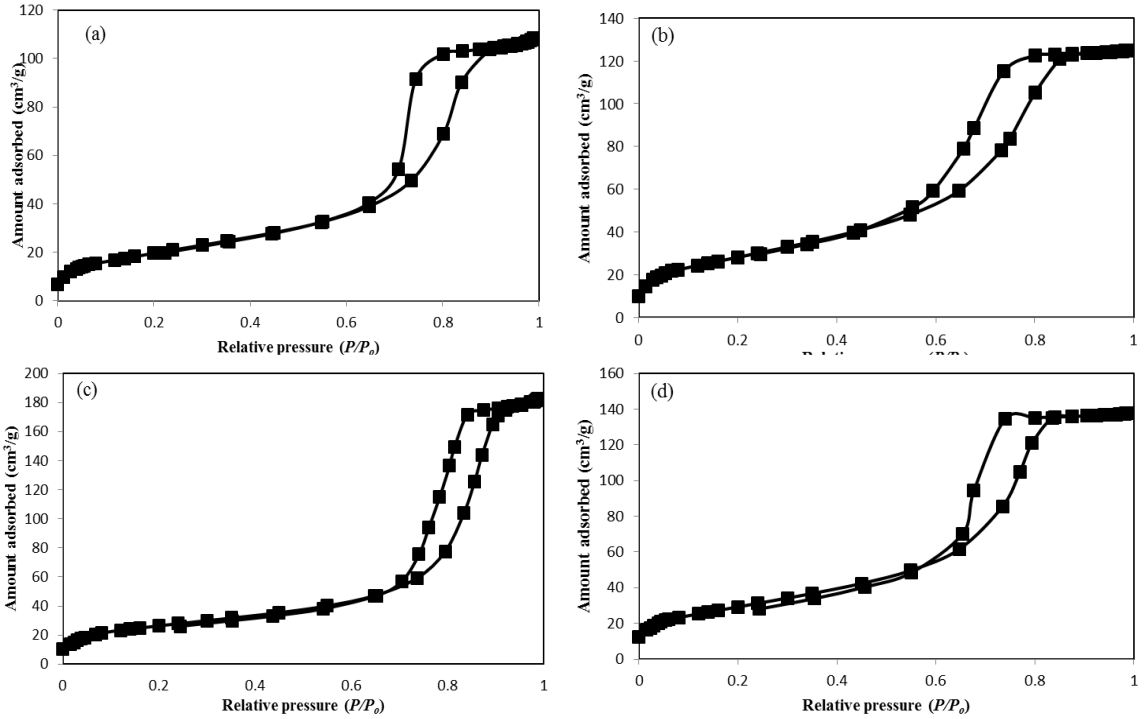

Figure 4. Physisorption isotherms for (a) 1wt%, (b) 2wt%, (c) 3wt% and (d) 5wt% Ce/TiO_2

N_2 adsorption isotherms of Ce/TiO_2 are type IV isotherms with H2-type hysteresis loops based on the IUPAC classification. H2 hysteresis loop are typical for mesoporous material. The difference in the mechanism of adsorption and desorption causes the main cavity becomes larger than the neck size distribution, with shape like an ink bottle [27][28].

BET surface areas (S_{BET}), pore volume (V_p) and pore diameter (D_p) and band gap energy showed in **Table 2.** Ce-doped TiO_2 exhibits larger catalyst surface areas compared TiO_2 pure, an advantageous trait for photocatalytic performance. The surface area TiO_2 pure is 88.7 m^2/g then BET surface area increases to be 141.98 m^2/g with addition of Ce concentration. Band gap energy values between 2.71 to 3.15 and the best response observed in Ce/TiO_2 with 5wt% concentration.

Table 2. Textural and optical properties of Ce doped TiO_2 photocatalysts

Photocatalyst	Textural			Band Gap (eV)
	S_{BET} (m^2/g)	V_{total} (cm^3/g)	Pore Diameter (Å)	
TiO_2	75.71	0.125	53.19	3.15
1wt% Ce/TiO_2	88.77	0.166	60.90	3.05
2wt% Ce/TiO_2	102.97	0.193	75.83	2.88
3wt% Ce/TiO_2	141.98	0.281	77.16	2.75
5wt% Ce/TiO_2	107.03	0.213	79.52	2.71

Based on the data in **Table 2.** Pure TiO_2 and Ce/TiO_2 with 1wt% concentration have a small BET surface area and ineffective for MB absorption. Ce/TiO_2 with 2wt% and 5wt% concentration has a large BET surface area, but the volume of small pores causes MB absorption becomes less effective. While, Ce/TiO_2 with 3wt% concentration has BET surface area and pore volume are larger, thus, MB absorption ability better than others. The addition of Ce with 3wt% concentration is best TiO_2 doping to increase the BET surface area and pores.

5. Photocatalytic dye degradation using Ce/TiO_2 photocatalysts

Photocatalytic activity of pure TiO_2 and Ce/TiO_2 photocatalyst under UV visible light irradiation are showed in **Figure 5.** The addition of Ce doping into TiO_2 increased the rate degrade of MB compared to with pure TiO_2.

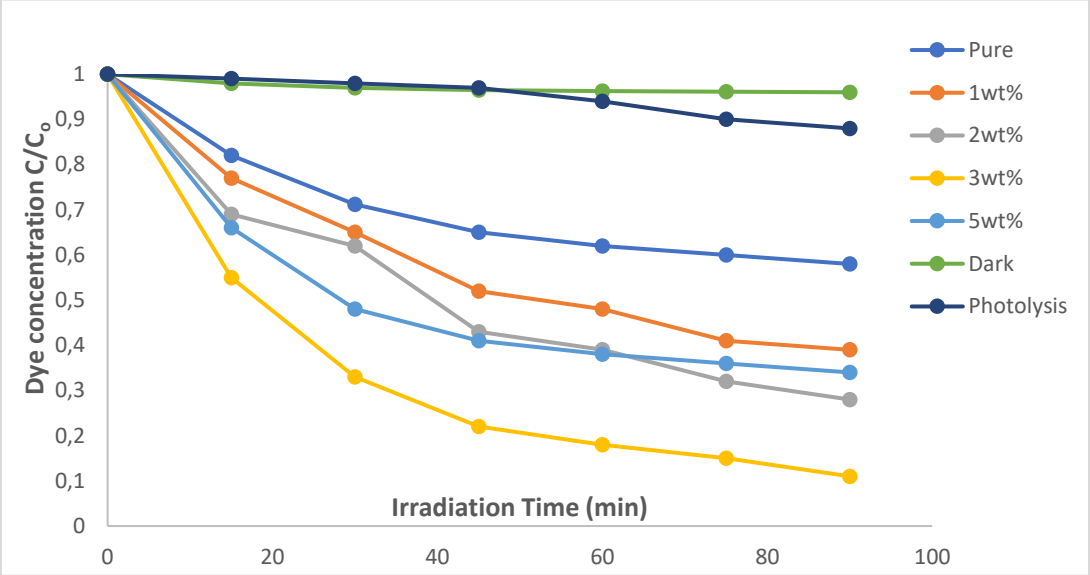

Figure 5. Photocatalytic activity of pure TiO_2 and Ce/TiO_2 photocatalyst Under UV-visible irradiation

These result show that the degradation rate increases with the addition Ce concentration. On other hand, the addition of Ce concentration further causes a decreased photocatalytic ability [10] and the rate the MB degradation. It is Indicates that excessive doping moved the dopant to the center of electron recombination [29]. Based on the experiment, 3wt% Ce doping proved to be the optimal dopant concentration for the doping of TiO_2, compared to the pure, 1wt%, 2wt% and 5wt% concentration. These result show that 3wt% of Ce/TiO_2 achieved the best performance under UV visible light irradiation. According to [3] that doping with Ce significantly enhancement the sensitivity of TiO_2 by reduces band gap energy and enhancement absorption under visible light or sunlight. Decrease of the band gap energy and enhancement the absorption was showed in **Table 2**. and **Figure 2.**

Photocatalytic activity of Ce doped TiO_2 was higher compared TiO_2 caused the increased of electrons and holes separation, it is indicated with the decreased of intensity the photoluminescence spectra in **Figure 3.** The Ce was capable to enhance center of

non-radiative oxygen defect. The enhance of defect sites enhancement the possibility of non-radiation energy transfer in the channel and trap the excited electrons for longer. thereby, reduced the possibility recombination of charge carriers and decreased PL intensity[30].

The Addition of cerium into TiO_2 prevent of surface hydroxyl groups to disappearance in while calcination process. the electron combined with O_2 and produce superoxide radical, electron holes reacted with hydroxyl ion to becomes hydroxyl radical and then oxidize of molecules [30]. Thereby, enhance the conductivity, electron transfer and reduced electron recombination under UV visible light irradiation. The best MB photodegradation reached 98.9% at a concentration 3wt% of Ce/TiO_2 with the end point of 0.11. This effectiveness because Ce doping into TiO_2, that decrease of crystal size, increases in surface area and decreases the recombination rate of electrons and holes. In addition, effect from degradation is the color of MB solutions becomes less intense or fade away.

CONCLUSION

TiO_2 is an effective of a catalyst that used to degradation of textile dye because of low-toxicity, chemical stability and environmentally friendly. The characterization results showed that Ce was successfully synthesized into the lattice structure of TiO_2 through sol gel method. The addition of Ce improved the light absorption ability and caused a red shift in the edge the photocatalyst absorption. The improved photocatalytic activity of Ce/TiO_2 could be associated to the large surface area and the enhanced inhibition of electron and holes recombination rates such as showed with reduced the PL spectrum intensity.

Based on the observed that the structure and activity of the photocatalysts affected by the Ce doping. when the Ce concentration in the catalyst increased then BET surface area increased and cause reduced the TiO_2 crystal size. The band gap of TiO_2 reduced and make the catalyst more reactive to the UV visible light irradiation. In addition, effect from degradation is the color of MB solutions becomes fades until achieved 98.9%. Thus, doping of Ce/TiO_2 is an effective method for degradation of MB.

This study found 12 genera from the order Orthoptera. The diversity of Orthoptera at ITERA was categorized as moderate, with the diversity index (H') values recorded as follows: Station I - 1.879, Station II - 1.765, Station III - 1.626, and Station IV - 1.843. No dominant individuals were found at any station. The evenness index at ITERA was categorized as high, with values of 0.784 at Station I, 0.767 at Station II, 0.678 at Station III, and 0.742 at Station IV, where Station I had the highest evenness value.

REFERENCES

[1] F. M. D. Chequer, G. A. R. de Oliveira, E. R. A. Ferraz, J. C. Cardoso, M. B. Zanoni, and D. P. de Oliveira, "Textile dyes: dyeing process and environmental impact," *Eco-friendly Text. Dye. Finish.*, vol. 6, no. 6, pp. 151–176, 2013.

[2] C. J. Ogugbue and T. Sawidis, "Bioremediation and detoxification of synthetic wastewater containing triarylmethane dyes by Aeromonas hydrophila isolated from industrial effluent," *Biotechnol. Res. Int.*, vol. 2011, no. 1, p. 967925, 2011.

[3] S. N. B. Saiful Amran, V. Wongso, N. S. Abdul Halim, M. K. Husni, N. S. Sambudi, and M. D. H. Wirzal, "Immobilized carbon-doped TiO2 in polyamide fibers for the degradation of methylene blue," *J. Asian Ceram. Soc.*, vol. 7, no. 3, pp. 321–330, 2019.

[4] S. Natarajan, H. C. Bajaj, and R. J. Tayade, "Recent advances based on the synergetic effect of adsorption for removal of dyes from waste water using photocatalytic process," *J. Environ. Sci.*, vol. 65, pp. 201–222, 2018.

[5] Y. D. Hou *et al.*, "N-doped SiO2/TiO2 mesoporous nanoparticles with enhanced photocatalytic activity under visible-light irradiation," *Chemosphere*, vol. 72, no. 3, pp. 414–421, 2008.

[6] F. Ansari *et al.*, "Novel nanostructured electron transport compact layer for efficient and large-area perovskite solar cells using acidic treatment of titanium layer," *Nanotechnology*, vol. 29, no. 7, p. 75404, 2018.

[7] X. Chen and S. S. Mao, "Titanium dioxide nanomaterials: synthesis, properties, modifications, and applications," *Chem. Rev.*, vol. 107, no. 7, pp. 2891–2959, 2007.

[8] K. Hashimoto, H. Irie, and A. Fujishima, "TiO2 photocatalysis: a historical overview and future prospects," *Jpn. J. Appl. Phys.*, vol. 44, no. 12R, p. 8269, 2005.

[9] M. R. Al-Mamun, S. Kader, M. S. Islam, and M. Z. H. Khan, "Photocatalytic activity improvement and application of UV-TiO2 photocatalysis in textile wastewater treatment: A review," *J. Environ. Chem. Eng.*, vol. 7, no. 5, p. 103248, 2019.

[10] Y. Nam, J. H. Lim, K. C. Ko, and J. Y. Lee, "Photocatalytic activity of TiO 2 nanoparticles: a theoretical aspect," *J. Mater. Chem. A*, vol. 7, no. 23, pp. 13833–13859, 2019.

[11] X. Li, H. Zhang, X. Zheng, Z. Yin, and L. Wei, "Visible light responsive NF-codoped TiO2 photocatalysts for the degradation of 4-chlorophenol," *J. Environ. Sci.*, vol. 23, no. 11, pp. 1919–1924, 2011.

[12] Z. He *et al.*, "A visible light-responsive iodine-doped titanium dioxide nanosphere," *J. Environ. Sci.*, vol. 23, no. 1, pp. 166–170, 2011.

[13] Y. Liu *et al.*, "Simulated-sunlight-activated photocatalysis of Methylene Blue using cerium-doped SiO2/TiO2 nanostructured fibers," *J. Environ. Sci.*, vol. 24, no. 10, pp. 1867–1875, 2012.

[14] U. G. Akpan and B. H. Hameed, "The advancements in sol–gel method of doped-TiO2 photocatalysts," *Appl. Catal. A Gen.*, vol. 375, no. 1, pp. 1–11, 2010.

[15] S. SAKAI, S. KUROKI, T. OBA, and T. SUZUKI, "Synthesis optimization and characterization of visible-light responsive Ce-doped titanate nanotubes for enhanced degradation of polluting dyes in aqueous environment," *Environ. Control Biol.*, vol. 54, no. 1, pp. 71–74, 2016.

[16] C. Fan, P. Xue, and Y. Sun, "Preparation of nano-TiO2 doped with cerium and its photocatalytic

activity," *J. Rare Earths*, vol. 24, no. 3, pp. 309–313, 2006.
[17] N. Aisah, D. Gustiono, V. Fauzia, I. Sugihartono, and R. Nuryadi, "Synthesis and enhanced photocatalytic activity of Ce-doped zinc oxide nanorods by hydrothermal method," in *IOP conference series: materials science and engineering*, 2017, vol. 172, no. 1, p. 12037.
[18] M. Meksi, H. Kochkar, G. Berhault, and C. Guillard, "Effect of cerium content and post-thermal treatment on doped anisotropic TiO2 nanomaterials and kinetic study of the photodegradation of formic acid," *J. Mol. Catal. A Chem.*, vol. 409, pp. 162–170, 2015.
[19] M. Myilsamy, M. Mahalakshmi, V. Murugesan, and N. Subha, "Enhanced photocatalytic activity of nitrogen and indium co-doped mesoporous TiO2 nanocomposites for the degradation of 2, 4-dinitrophenol under visible light," *Appl. Surf. Sci.*, vol. 342, pp. 1–10, 2015.
[20] C.-H. Lee, J.-L. Shie, Y.-T. Yang, and C.-Y. Chang, "Photoelectrochemical characteristics, photodegradation and kinetics of metal and non-metal elements co-doped photocatalyst for pollution removal," *Chem. Eng. J.*, vol. 303, pp. 477–488, 2016.
[21] X. Lin, F. Rong, X. Ji, and D. Fu, "Carbon-doped mesoporous TiO2 film and its photocatalytic activity," *Microporous Mesoporous Mater.*, vol. 142, no. 1, pp. 276–281, 2011.
[22] X.-K. Liu *et al.*, "Nearly 100% triplet harvesting in conventional fluorescent dopant-based organic light-emitting devices through energy transfer from exciplex.," *Adv. Mater.*, vol. 27, no. 12, pp. 2025–2030, 2015.
[23] M. Nasir, S. Bagwasi, Y. Jiao, F. Chen, B. Tian, and J. Zhang, "Characterization and activity of the Ce and N co-doped TiO2 prepared through hydrothermal method," *Chem. Eng. J.*, vol. 236, pp. 388–397, 2014.
[24] M. B. Marami and M. Farahmandjou, "Water-Based Sol–Gel Synthesis of Ce-Doped TiO 2 Nanoparticles," *J. Electron. Mater.*, vol. 48, pp. 4740–4747, 2019.
[25] D. Rajamanickam and M. Shanthi, "Photocatalytic degradation of an azo dye Sunset Yellow under UV-A light using TiO2/CAC composite catalysts," *Spectrochim. Acta Part A Mol. Biomol. Spectrosc.*, vol. 128, pp. 100–108, 2014.
[26] J. Liqiang *et al.*, "Review of photoluminescence performance of nano-sized semiconductor materials and its relationships with photocatalytic activity," *Sol. Energy Mater. Sol. Cells*, vol. 90, no. 12, pp. 1773–1787, 2006.
[27] P. C. S. Bezerra *et al.*, "Synthesis, characterization, and photocatalytic activity of pure and N-, B-, or Ag-doped TiO2," *J. Braz. Chem. Soc.*, vol. 28, no. 9, pp. 1788–1802, 2017.
[28] J. H. Page, J. Liu, B. Abeles, E. Herbolzheimer, H. W. Deckman, and D. A. Weitz, "Adsorption and desorption of a wetting fluid in Vycor studied by acoustic and optical techniques," *Phys. Rev. E*, vol. 52, no. 3, p. 2763, 1995.
[29] C. H. Nguyen, C.-C. Fu, and R.-S. Juang, "Degradation of methylene blue and methyl orange by palladium-doped TiO2 photocatalysis for water reuse: Efficiency and degradation pathways," *J. Clean. Prod.*, vol. 202, pp. 413–427, 2018.
[30] B. Choudhury, B. Borah, and A. Choudhury, "Extending photocatalytic activity of TiO2 nanoparticles to visible region of illumination by doping of cerium," *Photochem. Photobiol.*, vol. 88, no. 2, pp. 257–264, 2012.